

RESEARCH ARTICLE

Compressive Strength and Elastic Modulus of a 3D Woven Glass/Polyester Fire-Retardant Sandwich Composite

R. Hidayanto¹, D. I. Taufiq¹, H. Judawisastra^{2*}, and R. Wirawan^{2*}¹Study Program of Materials Science and Engineering, Faculty of Mechanical and Aerospace Engineering, Institut Teknologi Bandung, Jl. Ganesha No.10 Bandung Indonesia²Research Group of Materials Science and Engineering, Faculty of Mechanical and Aerospace Engineering, Institut Teknologi Bandung, Jl. Ganesha No. 10 Bandung 40132, Indonesia

ABSTRACT - A 3D woven sandwich composite structure has been widely used in various fields due to its advantages in terms of its strength-to-weight ratio. The adoption of lightweight materials in the railway industry for train carriages is aligned with United Nations Sustainable Development Goal 11, as this fosters the development of sustainable transportation by reducing carriage weight, enhancing fuel efficiency, minimizing component wear, and mitigating air pollution. This study explores the effect of the addition of aluminum trioxide (ATH) filler on the core structure, density, compressive strength, elastic modulus, and the number of added layers of 3D woven core fabric with 2D woven face sheets. Sandwich composites were produced with varying ATH loads of 30%, 40%, and 50%. We also varied the number of 3D woven core fabric layers in the composite sandwich (one, two, three, and four layers) and the 2D preform (one on the upper side, two on the upper side, and one on the upper + two on the lower sides) used as a face sheet thickener. The results showed that the addition of ATH filler increased the composite density. The addition of up to 40% ATH improved the strength and elastic modulus of the composite, while excessive loading led to a decrease in both properties. Variation of the 3D and 2D preform layers also improved the compressive strength and elastic modulus. We conclude that 3D woven sandwich composites incorporating 40% ATH, multilayered 3D woven core fabric, and 2D woven fabric face sheet thickener represent promising materials for use in the railway industry.

ARTICLE HISTORYReceived : 13th May 2023Revised : 16th Nov. 2023Accepted : 13th Dec. 2023Published : 20th Mar. 2024**KEYWORDS***3D woven sandwich composite**Compressive strength**Elastic modulus**Aluminum trioxide**Composite density**Failure mode*

1.0 INTRODUCTION

Sandwich composites are a structural composite group with high bending stiffness and strength, and low density [1, 2]. They find an extensive range of applications in the aerospace, automotive, and railway industries [3-5]. In the railway industry, the implementation of lightweight materials for train carriages contributes to a reduction in weight, which results in better fuel efficiency, reduced wear of components, and lower air pollution. This approach complies with the United Nations Sustainable Development Goal (SDG) 11, which is related to sustainable transportation [6, 7].

A sandwich composite has a structure consisting of two layers of skin with high stiffness and a low-density core layer. It offers excellent thermal and acoustic insulation, with energy absorption and low cost. However, the sandwich structure has certain drawbacks when it is subjected to shear, impact, and bending load, which result in skin delamination. To reduce the risk of this effect, a 3D woven sandwich fabric was invented, based on a fabric constructed from two parallel skin layers which are connected with vertical woven piles. The connection between the skin and the core gives improved delamination resistance to the sandwich structure [8-11].

Several studies have been conducted to investigate the mechanical performance of 3D woven sandwich composites. A 3D woven glass-epoxy sandwich containing polyurethane foam was shown to have excellent fatigue performance by Judawisastra et al. [12]. Bannister et al. conducted an experiment on a 3D woven sandwich combined with a foam core, and their results showed that the flatwise compression, edgewise compression, climbing drum peel, and flexural strength were significantly increased, due to the mutual reinforcement of the pile yarns and foam core [13]. Safari et al. studied a 3D woven sandwich composite with a nanostructured zeolite/polyurethane foam core to explore the response to flatwise compression, edgewise compression, three-point bending, and drop weight impact. Their findings indicated a notable enhancement in flexural strength, ultimate load, and energy absorption [14].

Mengyuan et al. conducted experiments in which they varied the 3D woven fabric, with core heights of 10 mm and 20 mm. Their results showed that the flexural properties of 3D woven sandwich composites increased with the core height, whereas the flat compression and shear properties decreased [15]. As the pile height increases, the compression strength of a 3D woven sandwich composite is reduced [16]. However, the use of a multi-layered 3D woven fabric improves the compression response and energy absorption of a 3D woven sandwich composite [17]. Thickening the facesheet of a sandwich composite by adding 2D fabric plies has been found to increase the flatwise and edgewise compressive strength of a 3D woven sandwich composite [18, 19].

In order to ensure that they can be used safely in transportation applications, polymeric materials require improved fire retardancy, and several approaches have been used to enhance this quality [8]; for example, fire retardant treatments have been applied to glass fabric and resin, and coating at the surface has been used to contribute to fire retardancy. The fire retardant coating increases the time to failure by slowing down the firing rate [3]. Javid et al. conducted experiments by treating carbon fiber reinforcements with phosphoric acid, and loading ammonium polyphosphate onto the epoxy resin. As a result, the performance of the manufactured sandwich composites against fire was found to be enhanced [20].

Aluminum trihydroxide (Al(OH)₃) (ATH) is well-known as a mineral filler material and is often loaded into a matrix to enhance fire retardancy [8, 21]. ATH is recognized for its low cost and non-toxicity [22]. Samyn et al. investigated the fire retardancy of a lightweight sandwich composite based on unsaturated polyester resin, glass fiber skins, and nonwoven polyester core material, with ATH used as a fire-retardant filler. The ATH loading in the matrix was shown to enhance the fire retardancy performance of the material [21]. In work by Wirawan et al., the loading of up to 40% ATH on 3D woven sandwich glass-polyester led to higher fire resistance [8].

Petersen et al. studied the effect of ATH loading on the mechanical properties (including tensile, compressive, shear and flexural strength) of FRP CSM laminates. The results showed a reduction in the mechanical properties as the ATH loading increased [23]. These findings align with those of a review paper by Ramadan et al., which reported that in general, various flame-retardant additives such as ATH reduced the tensile and flexural strength of composites. However, by using a hybrid type of flame retardant, an improvement in the mechanical properties could be achieved [22]. Another study by Atiqah et al. investigated the effect of ATH loading on kenaf-polyester composite laminates. An increase in mechanical properties was observed at 5% ATH due to good adhesion bonding between the fiber, resin, and ATH filler; however, beyond 5% ATH loading, a decrease in mechanical properties was evident due to an increase in the distribution and size of pores, which affected the cohesion bonding between the fiber, resin, and ATH filler [24]. In other words, there is an optimum point for the strengthening effect of ATH in composite laminate.

From the above discussion, it can be seen that loading ATH into the matrix effectively enhances the fire retardancy of polymeric composite materials. Furthermore, there is an optimum point for this effect in terms of improving the mechanical properties. However, the effects of ATH loading on the mechanical properties of 3D woven sandwich composites have not yet been explored. Thus, our work aims to investigate the influence of ATH loading, the number of 3D woven core fabric layers, and the number of 2D woven fabric layers used as facesheets on the density, compressive strength, and elastic modulus of 3D woven glass/polyester fire-retardant sandwich composite. In addition, we explore how the number of 3D woven core fabric layers and the number of 2D woven fabric layers used as facesheets affect the flatwise compressive strength and the elastic modulus of 3D woven sandwich glass-polyester composites at 40% ATH loading. This research has considerable importance for the railway industry, as it involves the development of a 3D woven glass-polyester sandwich composite; this aligns with Sustainable Development Goal 11 by ensuring secure and sustainable mass transportation. A flammability test is not included in this work, as this has been reported elsewhere [8].

2.0 MATERIAL AND METHOD

2.1 Sample Preparation

Specimens of sandwich composite panels were fabricated using unsaturated polyester resin as a matrix, with methyl ethyl ketone peroxide (MEKP) as a curing agent and ATH filler as a fire retardant. The 3D woven core fabric was used as the core, and 2D woven roving as the facesheet. Detailed information on this material is shown in Table 1, and the material properties are presented in Table 2.

Table 1. Constituent materials for 3D woven sandwich composites

No.	Material	Type	Supplier	Country of origin
1	2D woven roving	Glass fibre	PT Justus Kimiaraya	China
2	3D woven core fabric	Glass fibre	Beihai Fiberglass Co., Ltd.	China
3	Unsaturated polyester resin	Yukalac 157 BQTN-EX	PT Justus Kimiaraya	Indonesia
4	ATH	ATH BW 153	PT Justus Kimiaraya	China
5	MEKP	Mepoxe A	PT Justus Kimiaraya	Indonesia

Table 2. Mechanical and physical properties of constituent materials

No.	Material	Properties
1	2D woven roving	Areal weight : 600 g/m ²
2	3D woven core fabric	Areal weight : 900 g/m ² Core height : 6 mm Warp density : 15 ends/cm Weft density : 10 ends/cm

Table 2. (cont.)

No.	Material	Properties
3	Unsaturated polyester resin	Tensile strength warp : 5500 n/50 mm
		Tensile strength weft : 9400 n/50 mm
		Specific gravity : 1.21±0.02 g/cm ³
		Hardness : 40 Barcol /GYZ 934-1
		Flexural strength : 55 N/mm ²
		Flexural modulus : 3000 N/mm ²
4	ATH	Young's modulus : 1.18 GPa
		Specific gravity : 2.4 g/cm ³
		Particle size : 15 μm

The 3D fabric was composed of two surfaces of woven fabric, linked mechanically through vertical woven piles. These vertical woven piles were formed from a combination of two S-shaped piles, forming a figure-eight pattern in the warp direction and a straight line in the weft direction. A 3D woven sandwich composite panel was fabricated from the 3D fabric using the hand lay-up method. The resin was manually impregnated into the preforms with the assistance of an aluminum roller, which was operated by hand. The impregnation process was conducted layer by layer, with each layer added on top of the previous one until the stacking sequence was fully achieved. The hand lay-up procedure was strictly conducted within the resin-catalyst mixture's pot life. The curing of the sandwich composite panel took place at room temperature for 24 hours.

Detailed sample and specimen codes are listed in Table 3, where the samples used for observation of the core structure are numbered 5 to 11, the samples used for the density tests are labeled 1 to 8, and the samples used for the flatwise compressive tests are labeled 5 to 15. The consolidation of layers during the hand lay-up process is illustrated in Figure 1(a), while the finished 3D woven sandwich composite is depicted in Figure 1(b).

Table 3. Samples used for density, flatwise compressive strength, and elastic modulus tests

No	Number of 3D preforms	Number of 2D preforms	Weight% ATH to polyester	Specimen code	Testing
1	-	2	0	WR.PS-ATH (0)	D
2	-	2	30	WR.PS-ATH (30)	D
3	-	2	40	WR.PS-ATH (40)	D
4	-	2	50	WR.PS-ATH (50)	D
5	1	-	0	3D.PS-ATH (0)	S, D, & C
6	1	-	30	3D.PS-ATH (30)	S, D, & C
7	1	-	40	3D.PS-ATH (40)	S, D, & C
8	1	-	50	3D.PS-ATH (50)	S, D, & C
9	1	-	40	3D(1).PS-ATH 40	S & C
10	2	-	40	3D(2).PS-ATH 40	S & C
11	3	-	40	3D(3).PS-ATH 40	S & C
12	4	-	40	3D(4).PS-ATH 40	C
13	3	1	40	3D(3).WR(1).PS-ATH 40	C
14	3	2	40	3D(3).WR(2).PS-ATH 40	C
15	3	1+2	40	3D(3).WR(1+2).PS-ATH 40	C

Note: S=Structure, D=Density, C=Compression

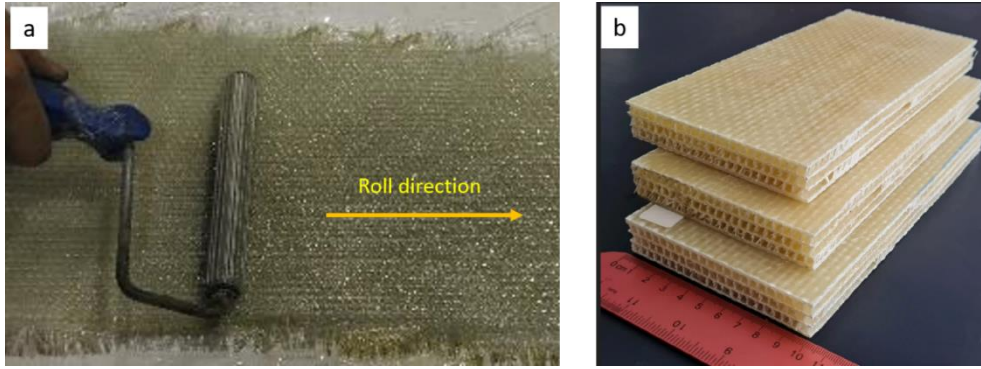


Figure 1. Manufacturing of 3D woven sandwich composites: (a) the hand lay up process; (b) final product.

2.2 Observation of the 3D Woven Sandwich Structure

A Nikon Eclipse 50i POL polarising stereo microscope was used to examine the core structure of the 3D woven sandwich in the warp and weft directions. The failure mode during the flatwise compression test was also observed using a stereo microscope.

2.3 Density of 3D Woven Sandwich Composites

The composite density was characterized using the ASTM C271 standard test method for the density of sandwich core materials. The specimens were cut to dimensions of 50 x 50 mm using a table saw, the thickness was measured using a digital vernier caliper, and their volumes were calculated using Eq. (1). The specimens were then weighed with a digital weighing scale, and the density of the 3D woven core was determined by dividing the mass of the specimen by the volume of the core material. The density of the 3D woven sandwich was calculated using Eq. (2).

$$V = l \times w \times h \quad (1)$$

where:

l = length of specimen, mm

w = width of specimen, mm

h = height of specimen, mm

V = volume of material, cm³

$$\rho = \frac{m}{V} \quad (2)$$

where:

ρ = density of material, g/cm³

m = mass of material, g

V = volume of material, cm³

2.4 Compressive Strength and Elastic Modulus

Flatwise compressive strength testing was conducted using an Instron UTM 6800 series (68FM-300). The specimens were cut to dimensions of 50 x 50 mm, with three specimens per test condition, following the ASTM C365 standard. This testing method involves subjecting a sandwich core to a uniaxial compressive force perpendicular to the plane of the facings, replicating its placement in a structural sandwich construction. The sandwich core was initially loaded with 45 N through the use of loading platens connected to the testing machine, and a displacement rate of 0.50 mm/min was applied. The force was continuously applied to the specimen until failure, or until the deflection reached 2% of the initial thickness of the specimen [25]. From the test results, we obtained force versus displacement data, meaning that the compressive strength of the 3D woven sandwich could be calculated using Eq. (3). The elastic modulus of the sample was obtained from the deflection shown in a compressive test, which was measured by a dial indicator. The elastic modulus of the 3D woven sandwich was calculated using Eq. (4) [26].

$$\sigma = \frac{P}{A} \quad (3)$$

where:

σ = core compressive strength, MPa (psi)

P = ultimate load, N (lb)

A = cross section area, mm² (in²)

$$E = \frac{St}{A} \quad (4)$$

where:

E = core compressive modulus, MPa (psi)

S = $\left(\frac{\Delta P}{\Delta \mu}\right)$, the slope of the initial linear portion of the load-deflection curve, N/mm (lb/in)

μ = displacement with respect to the two loading anvils, mm (in)

t = core thickness, mm (in)

3.0 RESULTS AND DISCUSSION

3.1 Observation of Core Structure of 3D Woven Sandwich Composites

The 3D woven sandwich composites were observed in order to study the effects of ATH loading and the use of three layers of 3D woven core fabrics on the core structures. The samples were coded as follows: one ply of 3D woven core fabric with ATH loading varied from 0–50% (3D.PS-ATH(x)), and three layers of 3D woven core fabrics with ATH loading of 40% (3D(3). PS-ATH 40), as listed in Table 3.

3.2 Single Ply 3D Woven Core Fabric with Variable ATH Loading from 0–50% (3D.PS-ATH(x))

For the 3D.PS-ATH(x) samples, Figure 3.(a) shows that with an increase in the addition of ATH to the weight of the polyester resin in the 3D woven sandwich, the area of the polyester resin covering the columns increases when observed from the warp direction. This is evident from the rise in the column widths with the addition of ATH weights ranging from 0% to 50% of the polyester resin weight. Figure 3.(a) shows that the loading of ATH filler in the polyester resin results in wider columns compared to when no ATH filler is present. However, there is no significant difference in column height when ATH weight is added to the polyester resin, as shown in Figure 2.(b).

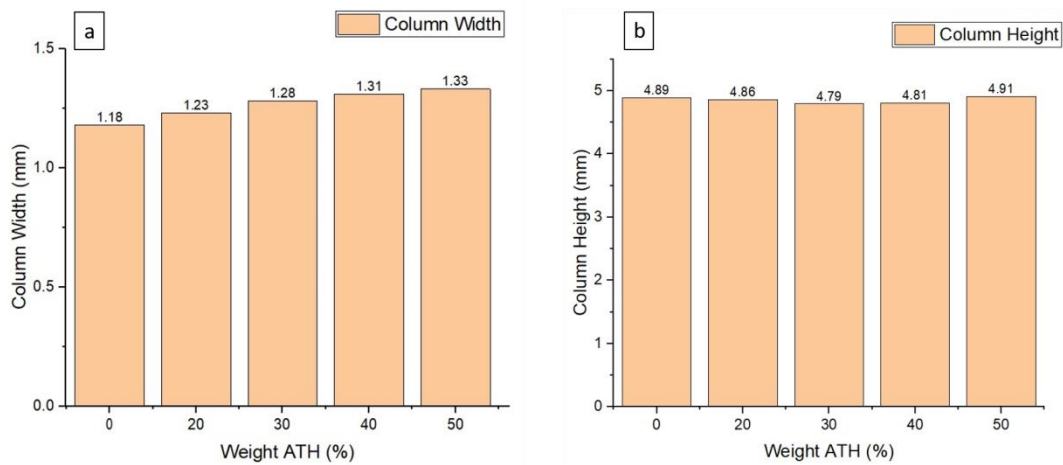


Figure 2. Construction of core sandwich dimension with ATH loading varying in the range 0–50%: (a) column width; (b) column height

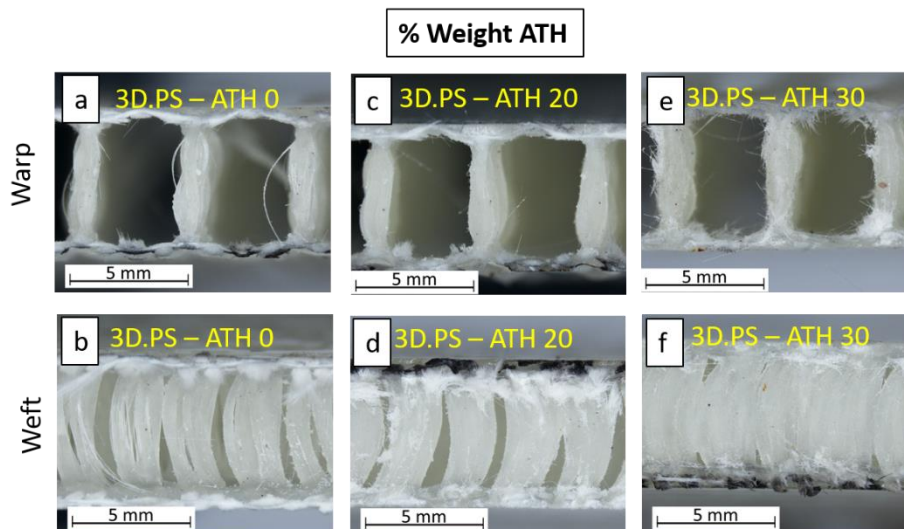


Figure 3. One layer of 3D woven fabric with varying ATH loading (3D.PS-ATH(x)): (a,b) 3D.PS-ATH(0) from warp and weft; (c,d) 3D.PS-ATH(20) from warp and weft; (e,f) 3D.PS-ATH(30) from warp and weft

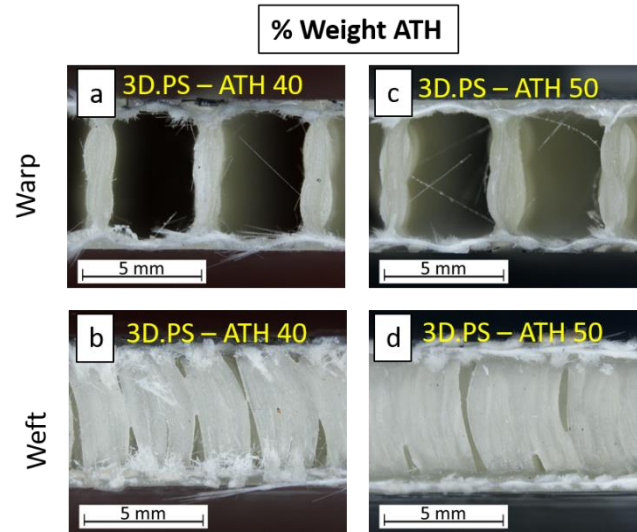


Figure 4. One layer of 3D woven fabric with varying ATH loading (3D.PS-ATH(x)): (a,b) 3D.PS-ATH(40) from warp and weft; (c,d) 3D.PS-ATH(50)

Figure 3 and 4 show that an increase in the proportion of ATH additive to the weight of resin in the 3D woven sandwich leads to the formation of more polyester resin networks when observed from the warp direction. It is notable that as the ATH weight increases from 0% to 50% of the resin weight, the void spaces between the columns decrease. The addition of ATH filler to the polyester resin creates fewer void spaces between the columns compared to the absence of ATH additive, which causes an increase in the column width. These results are in line with those of a study conducted by Atiqah et al., where the addition of ATH into the polymer matrix led to an increase in the size distribution and size of the pores, which caused an increase in the column width [24].

3.3 3D Woven Core Fabrics with Fixed ATH Loading 40% (3D(3).PS-ATH 40)

The sequence used in the manufacturing process of the composite panel was from the bottom to the top layer. The observations of the column width and height for the top, middle and bottom layers are presented in Figure 5. The results show that the column width for the 3D woven sandwich composite decreased from bottom to top, as illustrated in Figure 5(a). For the column height of (3D(3).PS-ATH 40), an increasing trend is shown from the bottom to the top (Figure 5(b)).

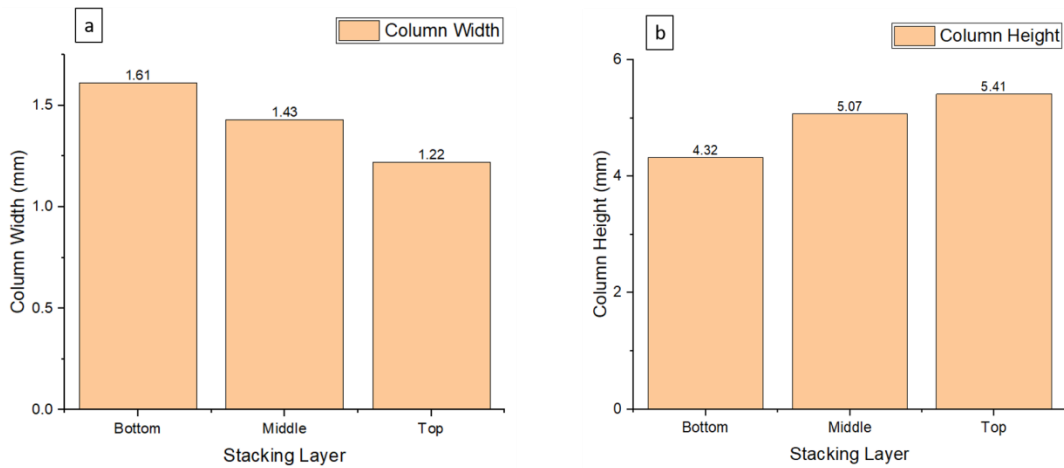


Figure 5. Results for stacked layers of (3D(3).PS-ATH 40): (a) column width; (b) column height

The top layer had the lowest column width and the greatest column height (Figure 6(b)). This was because the top layer was the last one applied in the lay up process, and the only force experienced was from roller consolidation. The middle layer had moderate values of the column width and column height (Figure 6(c)), as it experienced forces from both roller consolidation and top layer consolidation. The bottom layer had the highest column width and the lowest column height (Figure 6(d)), as this layer underwent roller consolidation three times, and the weight of the resin made the core height lower than that of the actual fabric [27]. We note that the pile yarn tilts, due to the force applied during the process. This tilt of the pile yarns, as shown in Figure 7(a–d), is the reason for the lowest height in the bottom layer.

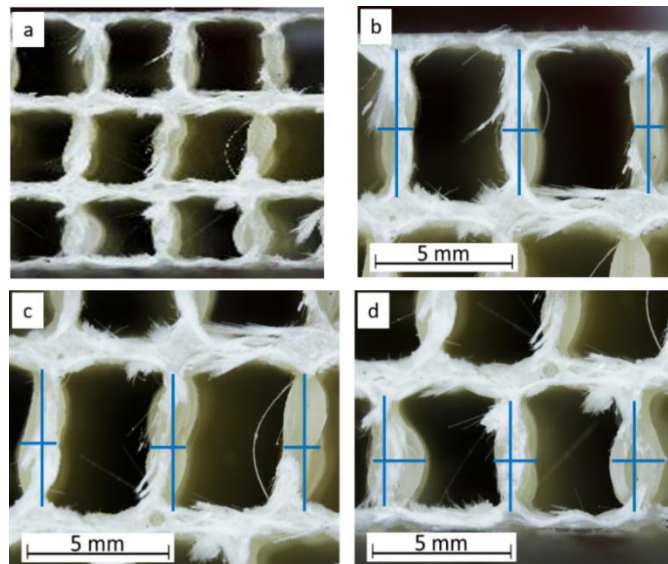


Figure 6. Microscope stereo observations from the warp direction of 3D woven sandwich with 40% ATH: (a) three layers of 3D woven stacked material; (b), top layer of sandwich composite; (c) middle layer of sandwich composite; (d) bottom layer of sandwich composite

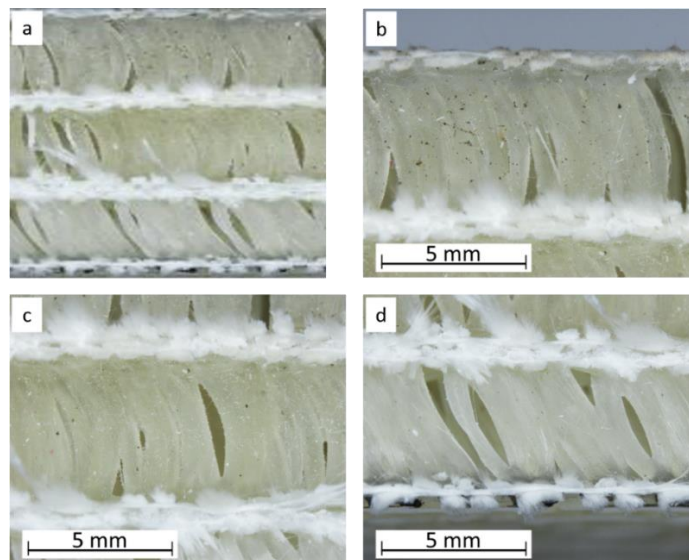


Figure 7. Microscope stereo observations from the weft direction of 3D woven sandwich with 40% ATH: (a) three layers of 3D woven stacked material; (b) top layer of sandwich composite; (c) middle layer of sandwich composite; (d) bottom layer of sandwich composite

3.4 Density of 3D vs 2D Woven Composite Sandwich

Fiber-reinforced plastic (FRP) has two main constituents: resin (used as a matrix) and fiber (used as reinforcement). Micromechanics has been used to predict the properties of FRP materials, as these are controlled by the volumes of fiber and matrix [28]. In the sample used for this experiment, ATH was added to the matrix to improve the fire retardancy, and 3D woven core fabric was used to achieve a lower mass [26]. The addition of ATH to the matrix affects the density of the composite [29], which differs significantly between the 2D solid composite and the 3D woven sandwich composite, as shown in Figure 8(a).

The density of 2D solid composite with 0% ATH was 1.74 g/cm^3 , which increased to 1.78, 1.8 and 1.82 g/cm^3 as the ATH content was increased to 30%, 40%, and 50%. It showed a positive trend in regard to the effect of the addition of ATH on the density.

The density of the 3D woven sandwich with 0% ATH was 0.48 g/cm^3 . As the ATH content was raised to 30%, 40%, and 50%, the density increased to 0.53, 0.55 and 0.58 g/cm^3 (Figure 8(b)). The difference in the density of the 2D solid composite and the 3D woven sandwich composite was 70%, which was due to the structure of the 3D woven preform creating a space in between the pile yarns, as shown in Figure 6. From the test results, we can draw the conclusion that loading ATH into the matrix provides an increase in the composite density, a finding that supports those of Barbero et al. and Aruniit et al. [28, 29].

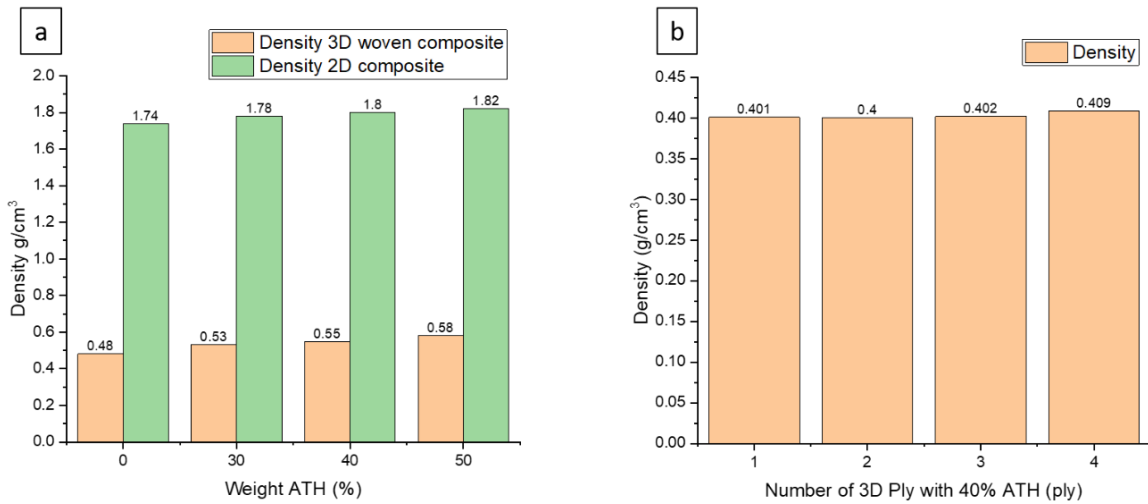


Figure 8. Density of 3D woven sandwich composite with variation in (a) % ATH; (b) number of layers

3.5 Effect on Composite Density of Adding 3D Woven Core Fabric

The effect of varying the number of 3D woven layers on the composite density with 40% ATH filler was also studied, as shown in Figure 8(b). With one ply of 3D woven fabric, the density was 0.401 g/cm³, and when the number was increased to two, three, and four plies, the density rose to 0.4, 0.402, and 0.409 g/cm³. These results showed that varying the number of layers of 3D woven fabric had no effect on the composite density. This was because the ATH content used as fire retardant filler in the matrix remained fixed at 40%. Hence, when the number of 3D woven core fabrics was varied, the composite density was unchanged, as there was no increase in the volume fraction of the main constituent [30].

3.6 Compressive Strength and Compressive Modulus for 3D(1).PS-ATH (x)

An FRP component must have adequate strength to ensure it does not break during service [31]. We therefore tested the compressive strength via a flatwise compression test. This test is important for composite sandwich structures, as the results represent the strength and stiffness of the sandwich panel when subjected to a perpendicular force [26]. Figure 9.(a) describes the effect of loading ATH into a polyester matrix with proportions of 0%, 30%, 40% and 50%. An increase in the compressive strength was observed up to 40% ATH loading at 0.81 MPa; however, at 50% ATH loading, the compressive strength did not increase but instead decreased by 30% from 0.81 MPa to 0.7 MPa. This trend indicates that the optimum ATH loading was 40%.

The strengthening effect of ATH arises from optimal cohesion bonding among the fibers, resin, and matrix, which facilitates efficient stress transfer. However, loading ATH at 50% is excessive, resulting in reduced compressive strength, which can be attributed to the effect of the distribution and size of the pores adversely impacting the cohesion bonding between the fibers, resin, and ATH filler. Excessive ATH leads to agglomeration, which further weakens the bonding [24].

A similar trend can be seen for the compressive modulus with varying ATH loading of the matrix. At 40% ATH loading, a peak is seen in the compressive modulus, but at 50% ATH loading, the compressive modulus drops to 6%, as shown in Figure 9.(b). Modification of the matrix with ATH above 40% affects its strength and modulus, as these depend on several factors such as particle size, adhesion, and particle loading. Hence, the changes in the strength and modulus with the volume fraction of filler can be predicted [32]. These results are aligned with those of work by Wirawan et al., where the fire retardancy effect did not improve when loaded with 50% ATH [8].

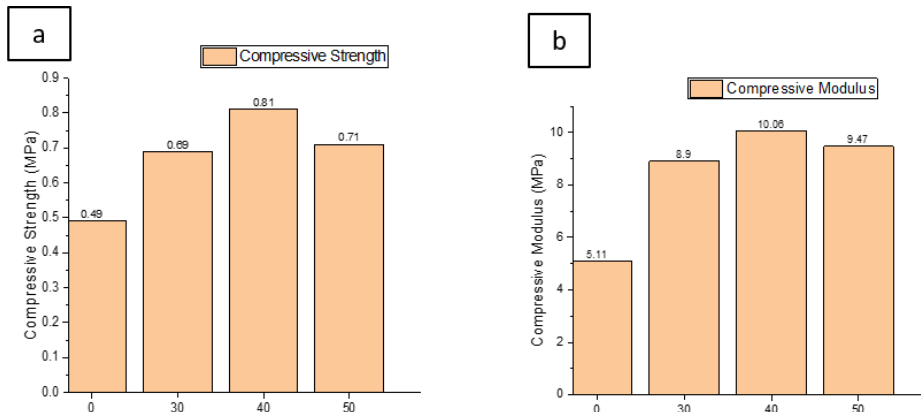


Figure 9. (a) Compressive strength and (b) compressive modulus of 3D(1).PS-ATH (0,30,40,50)

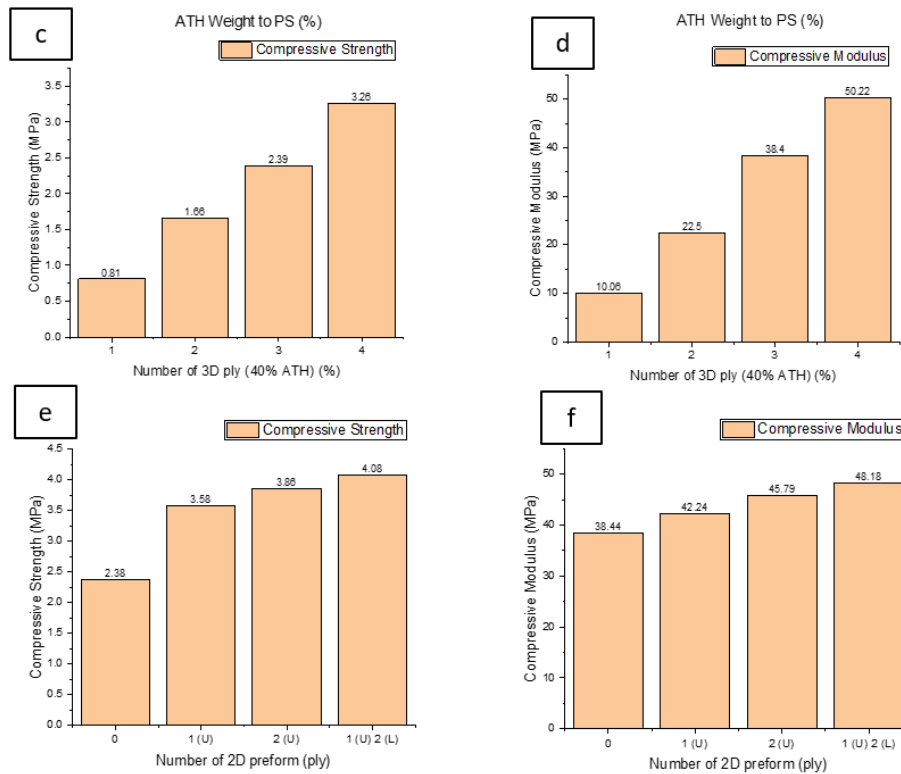


Figure 9. (cont.) (c) compressive strength and (d) compressive modulus of 3D(1,2,3,4).PS-ATH 40; (e) compressive strength and (f) compressive modulus of 3D(3).WR(0,1,2,1+2).PS-ATH 40

3.7 Compressive Strength and Compressive Modulus of 3D(x).PS-ATH 40

A loading of 40% ATH gave a compressive strength of 0.81 MPa, which was the optimum value and was achieved with one ply of 3D woven sandwich composite. This was also found to be the optimum content of ATH to improve fire retardancy in the study conducted by Wirawan et al. [8]. The number of 3D woven fabric layers was varied in order to observe whether this affected the compressive strength and elastic modulus of the 3D woven composite structure. Figure 9.(c) presents data on the compressive strength of the 3D woven composite sandwich with varying numbers of 3D woven core fabric plies. With two plies of 3D woven core fabric, the compressive strength was doubled, from 0.81 to 1.66 MPa. The compressive strength also increased 30% from 1.66 MPa to 2.39 MPa when three plies of 3D woven sandwich composite were used. With four plies, an increase was seen in the compressive strength from 2.39 MPa to 3.26 MPa.

The compressive modulus was also characterized for samples with a fixed content of 40% ATH and varying numbers of 3D woven core fabric plies. The compressive modulus of the composites increased from 10.06 MPa to 22.5, 38.4, and 50.22 MPa for one, two, three and four layers of 3D woven core fabric, respectively. The trend towards an increase in the compressive strength with an increase in the number of 3D woven core fabric plies was similar to that for the compressive modulus.

The strength of the 3D woven sandwich composite is obtained from the pile yarn used in its construction. The core height of a single layer of a 3D woven sandwich influences its strength: a larger core height will reduce the strength [11]. However, in this work, we used a 3D woven core preform with a core height of 6 mm and created the composite by stacking between one and four plies. This stacking of the 3D woven sandwich increases the compressive strength and modulus instead of reducing them. This phenomenon occurs because each layer contains a face sheet of woven fiber, and the large contact area of the face sheet creates a uniform load distribution [33]. The uniform load distribution of each stacking creates a plastic micro buckling of the pile yarn, which provides energy absorption that makes the compressive strength and elastic modulus increase [16]. In addition, stacking of the 3D woven core fabric increases the composite thickness, giving a higher moment of inertia and providing better material stability under compressive loading [34].

3.8 Compressive Strength and Compressive Modulus of 3D(3).WR(x).PS-ATH 40

Figure 9.(e) shows the compressive strength of three-layer 3D sandwich composites for varying numbers of 2D preform layers used as face sheet thickeners. Woven roving (600 g/m²) was used as the face sheets. There were four types of samples, as listed in Table 3.

Sample 3D(3).WR(0).PS-ATH 40 had a compressive strength of 2.38 MPa, whereas 3D(3).WR(1).PS-ATH 40 had a compressive strength of 3.58 MPa. When the face sheet consisted of two layers of woven roving, the compressive strength increased to 3.86 MPa for 3D(3).WR(2).PS-ATH 40, and reached 4.08 for 3D(3).WR(1+2).PS-ATH 40. This was because the vertical figure-of-eight-shaped core piles act like numerous interconnected small curved rods. These rods serve as the

primary load-bearing elements, and when their capacity is surpassed, they undergo brittle shear fracture by abruptly snapping. Due to the unified weaving of the face sheet and core fibers, transferring compression loads from the thickened face sheets to the core fibers becomes more challenging. As a result, the shear stress experienced by the core fibers is reduced, thereby enhancing the composite's load-bearing capability [35].

A similar trend can be seen for the compressive modulus of the 3D woven sandwich composites when additional face sheet layers are added (Figure 9.(f)). The increases in the compressive modulus were 8%, 7%, and 5% for each variation of face sheet thickener. The addition of a 2D woven roving facesheet thickener was therefore found to increase the elastic modulus, as reported by Shiah et al. [35].

The more layers added to the face sheet, the higher the compressive strength and elastic modulus achieved. It is clear that the addition of layers to the face sheet increases the compressive strength of 3D woven sandwich composites [18, 19, 27].

3.9 Failure Mechanism

During flatwise compressive tests of 3D woven core fabric 3D(3).PS-ATH 40 with variation in the 2D preforms used as face sheets (3D(3).WR(1+2).PS-ATH 40), the failure mechanism was observed with a stereo microscope. In the sample 3D(3).PS-ATH 40 in Figure 10.(a), failure occurred due to compression in combination with shear. At the early stage of compression, several fibers separated from the bundle to create a larger curvature radius, known as buckling. As compression continued, the joint between the pile yarn and the face sheet rotated and tilted, resembling a plastic hinge [27]. The buckling phenomenon was recorded on the stress-strain curve; it is seen as three peaks on the graph indicating the number of layers, as shown in Figure 11.(a).

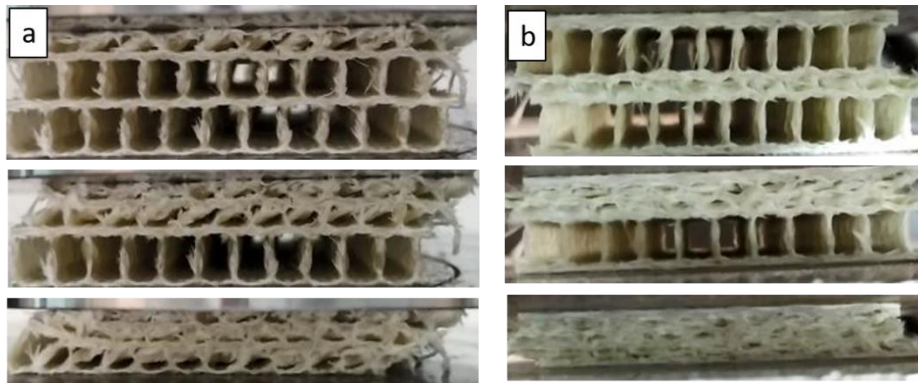


Figure 10. Microscope stereo observations for failure mode of samples: (a) 3D(3).PS-ATH 40; (b) 3D(3).WR(1+2)PS-ATH 40

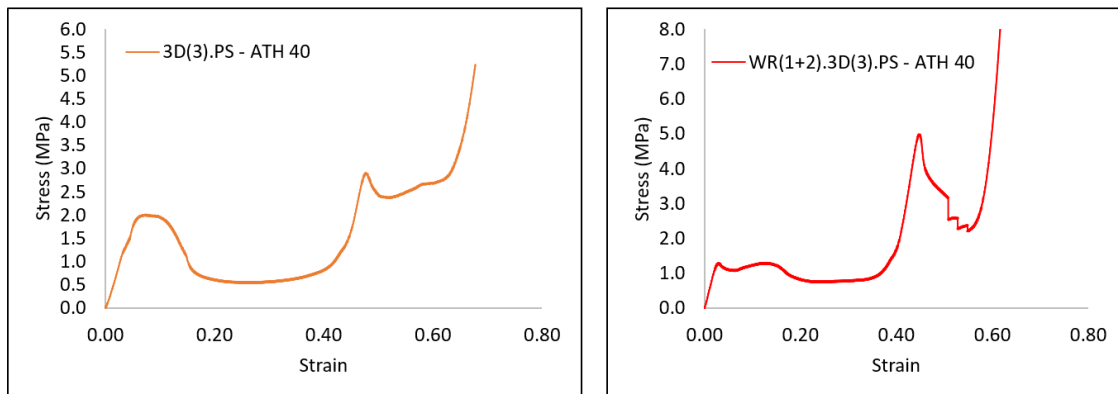


Figure 11. Stress strain curves for multi-layer 3D woven sandwich panel samples: (a) 3D(3).PS-ATH 40; (b) 3D(3).WR(1+2)PS-ATH 40

For the thickened facesheet of 3D woven sandwich composite 3D(3).WR(1+2)PS-ATH 40 (Figure 10.(b)), five peaks can be seen in the curve, as shown in Figure 11.(b). This is similar to the mode of failure for 3D(3).PS-ATH 40. The middle layer undergoes buckling and tilting, followed by the top and bottom layers. Once the layer has been completely crushed, densification starts and transmits the load, meaning that the curve subsequently rises. The peak shows a zigzag pattern rather than strain hardening (Figure 11.(b)) [17]. By comparing the curves for 3D(3).PS-ATH 40 and 3D(3).WR(1+2).PS-ATH 40, we see that the sample with 2D woven material as the facesheet has a notably higher peak. The compressive strength reaches 4.08 MPa, while for 3D(3).PS-ATH 40 it reaches only 3.26 MPa. These findings suggest that incorporating a 2D woven fabric as a thickener for the face sheet enhances the strength of the 3D woven sandwich composite, and is in line with those of previous works [18, 19].

4.0 CONCLUSIONS

The development of 3D woven composites for use in the railway industry can contribute to achieving sustainability in transportation and is aligned with SDG 11. This study has focused on investigating the effects of varying factors such as ATH loading, the number of 3D woven core fabric layers, and facesheet thickening techniques, to explore their effects on the core structure, density, compressive strength, and elastic moduli. Our experimental results lead to several key conclusions:

- The addition of ATH significantly influences the core structure of the 3D woven sandwich composite. The incorporation of ATH filler with polyester resin results in wider columns, although no notable change in column height is observed upon the addition of ATH weight to the polyester resin.
- In the specific case of a sample comprising three layers of 3D woven core fabric with a fixed ATH loading of 40% (3D(3).PS-ATH 40), the column width tends to broaden at the bottom layer and gradually narrows towards the top layer. This variation is attributed to the use of the hand lay-up process and the distribution of the resin weight.
- The inclusion of ATH in the matrix leads to an increase in composite density.
- Varying the loading of ATH from 0% to 40% gives an enhancement in both compressive strength and elastic modulus. However, a 50% ATH loading reduces the strength, due to excessive ATH causing agglomeration and weakening the bonding.
- The addition of a number of 3D woven core fabric layers and the incorporation of 2D woven fabric as a facesheet enhances both the compressive strength and elastic modulus.
- Finally, 3D woven sandwich composites with 40% ATH loading, multilayer 3D woven core fabric, and additional facesheets of 2D woven fabric show promise as materials for application within the railway industry.

5.0 ACKNOWLEDGEMENTS

This work was financially supported by the Ministry of Research, Technology and Higher Education Indonesia, through Kedaireka (*Matching Fund*) Program 2022-2023.

6.0 REFERENCES

- [1] W. D. Callister Jr and D. G. Rethwisch, *Callister's materials science and engineering*. Hoboken, NJ: John Wiley & Sons, 2020.
- [2] Y. Sun, L.C. Guo, T.S. Wang, S.Y. Zhong, and H.Z. Pan, "Bending behavior of composite sandwich structures with graded corrugated truss cores," *Composite Structures*, vol. 185, pp. 446-454, 2018.
- [3] A. Hörold, B. Schartel, V. Trappe, M. Korzen, and J. Bünker, "Fire stability of glass-fibre sandwich panels: The influence of core materials and flame retardants," *Composite Structures*, vol. 160, pp. 1310-1318, 2017.
- [4] N. Cadorin, R. Zitoun, P. Seitier, and F. Collombet, "Analysis of damage mechanism and tool wear while drilling of 3D woven composite materials using internal and external cutting fluid," *Journal of Composite Materials*, vol. 49, no. 22, pp. 2687-2703, 2015.
- [5] C. Pereszlai, N. Geier, D. I. Poor, B. Z. Balázs, and G. Póka, "Drilling fibre reinforced polymer composites (CFRP and GFRP): An analysis of the cutting force of the tilted helical milling process," *Composite Structures*, vol. 262, p. 113646, 2021.
- [6] J. Njuguna, *Lightweight composite structures in transport: Design, manufacturing, analysis and performance*. Cambridge Woodhead publishing, 2016.
- [7] Y.F. Li, W. Chen, and T.W. Cheng, "The sustainable composite materials in civil and architectural engineering," *Sustainability*, vol. 14, no. 4, p. 2134, 2022.
- [8] R. Wirawan, H. Judawisastra, and D. I. Taufiq, "Development of a fire-retardant 3-dimensional woven glass-polyester sandwich composite," in *AIP Conference Proceedings*, 2020, vol. 2262, no. 1: AIP Publishing LLC, p. 030012.
- [9] A. Jabbar, M. Karahan, M. Zubair, and N. Karahan, "Geometrical analysis of 3D integrated woven fabric reinforced core sandwich composites," *Fibres & Textiles in Eastern Europe*, vol. 27, no. 1, pp. 45-50, 2019.
- [10] B. Wang, B. Luo, R. Jiang *et al.*, "Double-layer woven lattice truss sandwich composite for multifunctional application: Design, manufacture and characterization," *Composites Part B: Engineering*, vol. 241, p. 110026, 2022.
- [11] M. Karahan, H. Gul, N. Karahan, and J. Ivens, "Static behavior of three-dimensional integrated core sandwich composites subjected to three-point bending," *Journal of Reinforced Plastics and Composites*, vol. 32, no. 9, pp. 664-678, 2013.
- [12] H. Judawisastra, J. Ivens, and I. Verpoest, "The fatigue behaviour and damage development of 3D woven sandwich composites," *Composite structures*, vol. 43, no. 1, pp. 35-45, 1998.
- [13] M. Bannister, R. Braemar, and P. Crothers, "The mechanical performance of 3D woven sandwich composites," *Composite Structures*, vol. 47, no. 1-4, pp. 687-690, 1999.
- [14] H. Safari, M. Karevan, and H. Nahvi, "Mechanical characterization of natural nano-structured zeolite/polyurethane filled 3D woven glass fiber composite sandwich panels," *Polymer Testing*, vol. 67, pp. 284-294, 2018.
- [15] M. Wang, H. Cao, and K. Qian, "Mechanical properties of three-dimensional fabric sandwich composites," *Journal of Engineered Fibers and Fabrics*, vol. 9, no. 3, p. 155892501400900301, 2014.

- [16] H. Fan, Q. Zhou, W. Yang, and Z. Jingjing, "An experiment study on the failure mechanisms of woven textile sandwich panels under quasi-static loading," *Composites Part B: Engineering*, vol. 41, no. 8, pp. 686-692, 2010.
- [17] H. Fan, W. Yang, and Q. Zhou, "Experimental research of compressive responses of multi-layered woven textile sandwich panels under quasi-static loading," *Composites Part B: Engineering*, vol. 42, no. 5, pp. 1151-1156, 2011.
- [18] D.S. Li, N. Jiang, L. Jiang, and C.Q. Zhao, "Static and dynamic mechanical behavior of 3D integrated woven spacer composites with thickened face sheets," *Fibers and Polymers*, vol. 17, no. 3, pp. 460-468, 2017.
- [19] V. Balakumaran, R. Alagirusamy, and D. Kalyanasundaram, "Epoxy based sandwich composite using three-dimensional integrally woven fabric as core strengthened with additional carbon face-sheets," *Journal of the Mechanical Behavior of Biomedical Materials*, vol. 116, p. 104317, 2021.
- [20] A. Javaid, H. T. Ashraf, M. Mustaghees, and A. Khalid, "Fire-retardant carbon/glass fabric-reinforced epoxy sandwich composites for structural applications," *Polymer Composites*, vol. 42, no. 1, pp. 45-56, 2021.
- [21] F. Samyn *et al.*, "Flame retardancy of lightweight sandwich composites," *Journal of Composites Science*, vol. 5, no. 10, p. 274, 2021.
- [22] N. Ramadan, M. Taha, A. D. La Rosa, and A. Elsabbagh, "Towards selection charts for epoxy resin, unsaturated polyester resin and their fibre-fabric composites with flame retardants," *Materials*, vol. 14, no. 5, p. 1181, 2021.
- [23] M. R. Petersen, A. Chen, M. Roll, S. Jung, and M. Yossef, "Mechanical properties of fire-retardant glass fiber-reinforced polymer materials with alumina tri-hydrate filler," *Composites Part B: Engineering*, vol. 78, pp. 109-121, 2015.
- [24] A. Atiqah, M. N. M. Ansari, M. S. S. Kamal, A. Jalar, N. N. Afeefah, and N. Ismail, "Effect of alumina trihydrate as additive on the mechanical properties of kenaf/polyester composite for plastic encapsulated electronic packaging application," *Journal of Materials Research and Technology*, vol. 9, no. 6, pp. 12899-12906, 2020.
- [25] ASTM Standard C365M-22. *Standard test method for flatwise compressive properties of sandwich cores*, ASTM International, West Conshohocken, PA, 2012 [Online]. Available: <http://www.astm.org/>
- [26] W. Ma and R. Elkin, *Sandwich structural composites: Theory and practice*. Boca Raton, FL: CRC Press, 2022.
- [27] L. Zhu, M. B. Rahman, and Z. Wang, "Effect of structural differences on the mechanical properties of 3D integrated woven spacer sandwich composites," *Materials*, vol. 14, no. 15, p. 4284, 2021.
- [28] E. J. Barbero, *Introduction to composite materials design*. Boca Raton, FL: CRC press, 2017.
- [29] A. Aruniit, J. Kers, and K. Tall, "Influence of filler proportion on mechanical and physical properties of particulate composite," *Agronomy Research Biosystem Engineering*, vol. 1, pp. 23-29, 2011.
- [30] G. Yerbolat, S. Amangeldi, M. H. Ali, N. Badanova, A. Ashirbeok, and G. Islam, "Composite materials property determination by rule of mixture and monte carlo simulation," in *2018 IEEE International Conference on Advanced Manufacturing (ICAM)*, Yunlin, Taiwan, 2018, vol. 18380687: IEEE, pp. 384-387.
- [31] F. L. Matthews and R. D. Rawlings, *Composite materials: engineering and science*. Boca Raton, FL: Woodhead Publishing, 1999.
- [32] M. Yossef and A. Chen, "A numerical model to study the effect of alumina tri-hydrate on mechanical properties of fiber reinforced polymers," in *Earth and Space 2016: Engineering for Extreme Environments*: American Society of Civil Engineers Reston, VA, 2016, pp. 858-868.
- [33] A. Malcom, M. Aronson, V. Deshpande, and H. Wadley, "Compressive response of glass fiber composite sandwich structures," *Composites Part A: Applied Science and Manufacturing*, vol. 54, pp. 88-97, 2013.
- [34] H. Nosraty, A. Mirdehghan, M. Barikani, and M. Akhbari, "Edgewise compression behavior of three-dimensional integrated woven sandwich composite panels," *Journal of Textiles and Polymers*, vol. 8, no. 2, pp. 53-63, 2020.
- [35] Y. C. Shiah, L. Tseng, J. C. Hsu, and J. H. Huang, "Experimental characterization of an integrated sandwich composite using 3D woven fabrics as the core material," *Journal of Thermoplastic Composite Materials*, vol. 17, no. 3, pp. 229-243, 2016.